Type I interferon negatively controls plasmacytoid dendritic cell numbers in vivo

Melissa Swiecki,[1] Yaming Wang,[1] William Vermi,[2] Susan Gilfillan,[1] Robert D. Schreiber,[1] and Marco Colonna[1]

[1]Department of Pathology and Immunology, Washington University School of Medicine, St Louis, MO 63110
[2]Department of Pathology, University of Brescia, 25121 Brescia, Italy

Plasmacytoid dendritic cells (pDCs) specialize in the secretion of type I interferons (IFN-I) and thus are considered critical mediators of antiviral responses. We recently reported that pDCs have a very early but limited and transient capacity to curtail viral infections. Additionally, pDC numbers are not sustained in human infections caused by Hepatitis B or C viruses (HBV and HCV) and HIV. Thus, the numbers and/or function of pDCs appear to be regulated during the course of viral infection. In this study, we show that splenic pDCs are reduced in vivo during several systemic viral infections and after administration of synthetic toll-like receptor ligands. We demonstrate that IFN-I, regardless of the source, contributes to this decline and mediates pDC death via the intrinsic apoptosis pathway. These findings demonstrate a feedback control mechanism by which IFN-I modulates pDC numbers, thus fine-tuning systemic IFN-I response to viruses. IFN-I–mediated control of pDCs may explain the loss of pDCs during human infections caused by HBV, HCV, or HIV and has important therapeutic implications for settings in which IFN-I is used to treat infections and autoimmune diseases.

CORRESPONDENCE
Marco Colonna
mcolonna@pathology.wustl.edu

Abbreviations used: DR5, death receptor 5; LCMV, lymphocytic choriomeningitis virus; MCMV, murine cytomegalovirus; pDC, plasmacytoid DC; p.i., post infection; poly(I:C), polyinosinic:polycytidylic acid; TLR, Toll-like receptor; TRAIL, TNF-related apoptosis-inducing ligand; VACV, vaccinia virus; VSV, vesicular stomatitis virus.

Plasmacytoid DCs (pDCs) are bone marrow–derived cells that specialize in the secretion of type I IFNs (IFN-I). pDCs detect RNA and DNA viruses through two endosomal sensors, toll-like receptor (TLR) 7 and TLR9, respectively, which induce secretion of IFN-I through the MyD88–IRF7 signaling pathway (Gilliet et al., 2008). IFN-I confers resistance to viral infections and promotes NK cell, DC, T cell, and B cell functions (García-Sastre and Biron, 2006). In addition to secreting IFN-I, pDCs produce IL-12, IL-6, and chemokines that contribute to innate and adaptive immune responses (Trinchieri, 2010). pDCs also express major histocompatibility complex and costimulatory molecules, and therefore may directly participate in presentation and cross-presentation of antigens to T cells (Villadangos and Young, 2008). Thus, pDCs have been implicated in both innate and adaptive immunity.

In mice, it has been reported that pDC numbers decline in spleens after TLR7/9 stimulation and during certain viral infections such as murine cytomegalovirus (MCMV) and lymphocytic choriomeningitis virus (LCMV; Asselin-Paturel et al., 2005; Zuniga et al., 2008; Lee et al., 2009). Decreased numbers of circulating pDCs have been observed in patients infected with Hepatitis B or C viruses (Duan et al., 2004; Kanto et al., 2004). pDC numbers are also reduced in the blood of patients infected with HIV. Loss of pDCs correlates with high viral load, decreased $CD4^+$ T cell counts, and the onset of opportunistic infections (Finke et al., 2004; Altfeld et al., 2011). At present, it is unclear what factors are responsible for the diminution of pDCs during human infections. pDCs could be direct targets of HIV because they express the HIV receptors and/or they may migrate into secondary lymphoid tissues where they undergo apoptosis by yet undefined mechanisms (Fonteneau et al., 2004; Malleret et al., 2008; Brown et al., 2009).

In this study, we investigated the turnover of pDCs in vivo during several systemic viral infections. We observed a marked reduction in splenic pDCs in infected mice, which inversely correlated with systemic levels of IFN-I. Viral infection induced the up-regulation of proapoptotic molecules in pDCs in an IFN-I–dependent manner resulting in caspase activation and death.

The Rockefeller University Press $30.00
J. Exp. Med. Vol. 208 No. 12 2367-2374
www.jem.org/cgi/doi/10.1084/jem.20110654

These findings unveil a novel feedback control mechanism by which IFN-I modulates pDC numbers in vivo for preventing excessive systemic IFN-I response to viruses.

RESULTS AND DISCUSSION

pDCs are reduced during systemic viral infections that induce IFN-I

To investigate the fate of pDCs during systemic viral infections, we infected C57BL/6 mice with disparate RNA or DNA viruses known to activate pDCs through the TLR7/9–MyD88–IRF7 pathway and monitored pDC numbers ($B220^+Siglec\text{-}H^+$ or $CD11c^+Siglec\text{-}H^+$) and systemic IFN-α levels at different time points post infection (p.i.). Flow cytometric analysis of spleens from HSV-1–infected mice revealed a decrease in pDCs compared with uninfected animals that was paralleled by an increase in serum IFN-α levels (Fig. 1 A). The reduced numbers of pDCs were not a result of the down-regulation of Siglec-H and therefore the inability to detect pDCs, as SiglecH-eGFP gene-targeted mice also had decreased numbers of GFP^+ pDCs after infection with HSV-1 (unpublished data). HSV-1 infection in other mouse strains also led to reduced numbers of pDCs, suggesting that the decline of pDCs after systemic virus infection is not strain dependent (unpublished data).

Infection with vesicular stomatitis virus (VSV) expressing OVA (VSV-OVA) or MCMV also resulted in the reduction of splenic pDCs during the first few days of infection when IFN-α levels were abundant in the serum (Fig. 1, B and C). To corroborate our flow cytometry data, we evaluated pDC numbers in spleens by histology. Frozen tissue sections of spleens obtained from control and MCMV-infected (36 h p.i.) mice stained with anti–Siglec-H showed numerous pDCs, mainly located in the white pulp (Fig. 1 D). Consistent with flow cytometry data, we found a significant reduction in the number of pDCs in MCMV-infected mice (Fig. 1 D). Lack of pDCs was heterogeneous, with areas of white pulp almost completely devoid of $Siglec\text{-}H^+$ cells (Fig. 1 D). The residual pDC population was occasionally found to form microclusters surrounding the periarteriolar lymphoid sheets (unpublished data).

Interestingly, in mice lacking efficient NK cell responses to MCMV (129/SvJ), we observed increased levels of systemic IFN-α and a more profound reduction in pDC numbers compared with MCMV-infected C57BL/6 mice (Fig. 1 E). Infection with LCMV clone 13, which establishes a chronic infection in mice, caused a transient drop in splenic pDC numbers around the time when IFN-α concentrations peak in the serum (Fig. 1 F), consistent with previous results (Zuniga et al., 2008; Lee et al., 2009). Our data suggests that pDC numbers plummet when IFN-I levels are prevalent in the serum and begin to recover when systemic IFN-I is no longer detectable. Thus, IFN-I might contribute to the rapid decline of pDCs during certain viral infections. In support of this, infection with vaccinia virus (VACV) did not elicit high levels of systemic IFN-I or cause a dramatic reduction in pDC numbers (Fig. 1 G).

IFN-I signaling induces pDC activation and death in vivo

To test whether the decline in pDC numbers during infection was related to pDC activation, death, and/or IFN-I signaling, we infected WT and $IFNAR^{-/-}$ mice with HSV-1 and then assessed frequencies of splenic pDCs ($CD11c^+Siglec\text{-}H^+$) and their expression of PDC-TREM and caspase. PDC-TREM is an early activation marker expressed by pDCs that is induced

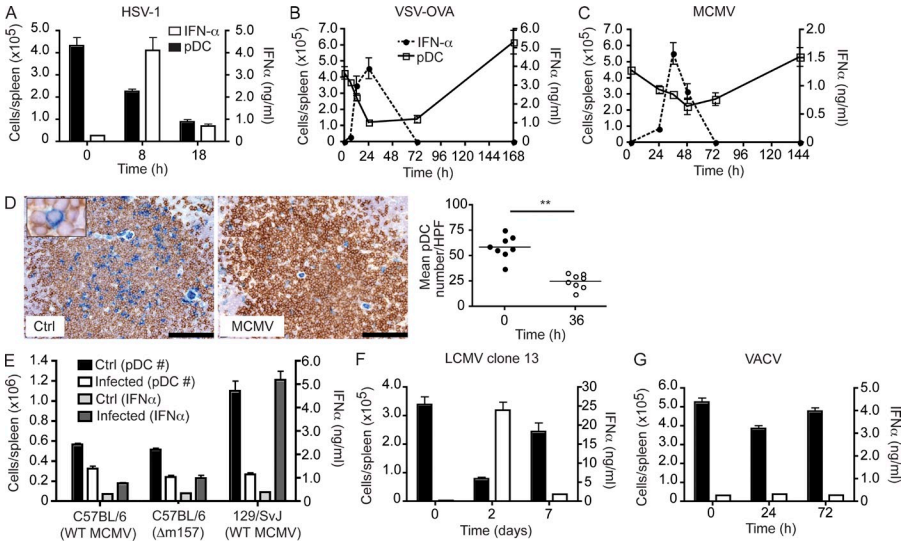

Figure 1. Decline of splenic pDCs during systemic viral infections. Mice were infected with RNA or DNA viruses and absolute numbers of pDCs and serum IFN-α levels were determined at different time points p.i. (A) C57BL/6 mice were infected with 10^7 pfu HSV-1. Data are representative of two experiments with four mice per time point. (B) C57BL/6 mice were infected with 5×10^6 pfu VSV-OVA. Data are representative of two experiments with four mice per time point. (C) C57BL/6 mice were infected with 5×10^4 pfu MCMV. Data are combined from two experiments with five to six mice per time point. (D) Spleen sections from uninfected (Ctrl) and MCMV-infected C57BL/6 mice were stained for Siglec-H (blue) and CD3 (brown). A magnification is shown in the inset. Bar, 100 µm. The graph shows mean pDC numbers per high power field (HPF) in Ctrl and MCMV-infected spleen sections ($n = 8$). (E) pDC numbers in spleens and serum IFN-α levels were determined from C57BL/6 (5×10^4 pfu MCMV; 10^4 pfu Δm157) and 129/SvJ (10^4 pfu MCMV) mice infected or not for 48 h ($n = 4$–5 mice per group). (F) C57BL/6 mice were infected with 3×10^6 pfu LCMV clone 13. Data are combined from two experiments with six to eight mice per time point. (G) C57BL/6 mice were infected with 2×10^6 pfu VACV. Data are representative of two experiments with three to five mice per time point. (A–C and E–G) Error bars represent means ± SEM. (A, F, and G) pDC numbers, black bars; IFN-α levels, white bars. (B and C) pDC numbers, open squares; IFN-α levels, closed circles. (D) Statistical significance is indicated by **, $P < 0.001$. Error bars represent means ± SD.

by TLR and IFN-I signaling (Watarai et al., 2008), whereas caspase activation is indicative of apoptosis. In HSV-1–infected WT mice, the frequencies of pDCs fell more than two-fold and those pDCs remaining expressed more PDC-TREM on the cell surface than pDCs from control mice (Fig. 2 A). Using a pan-caspase inhibitor that is an in situ marker for apoptosis, we found that ∼37% of pDCs from infected WT mice were caspase$^+$ compared with ∼11% in uninfected mice. In IFNAR$^{-/-}$ mice infected with HSV-1, the frequencies of splenic pDCs were comparable to uninfected IFNAR$^{-/-}$ mice (0.4 and 0.5, respectively) and there was no up-regulation of PDC-TREM or differences in caspase activation in pDCs from control and infected animals (Fig. 2 B).

Quantitative analysis of pDC numbers in control and HSV-1–infected mice revealed a greater reduction in WT mice compared with IFNAR$^{-/-}$ mice (Fig. 2 C). Concomitantly, when IFN-I signaling was blocked with anti-IFNAR mAb in WT mice before infection with HSV-1, pDC numbers and survival remained similar to those found in uninfected mice (Fig. 2 D). To validate that pDCs were in fact undergoing apoptosis in an IFN-I–dependent manner, we evaluated both caspase$^+$ and Annexin V$^+$ pDCs in WT and IFNAR$^{-/-}$

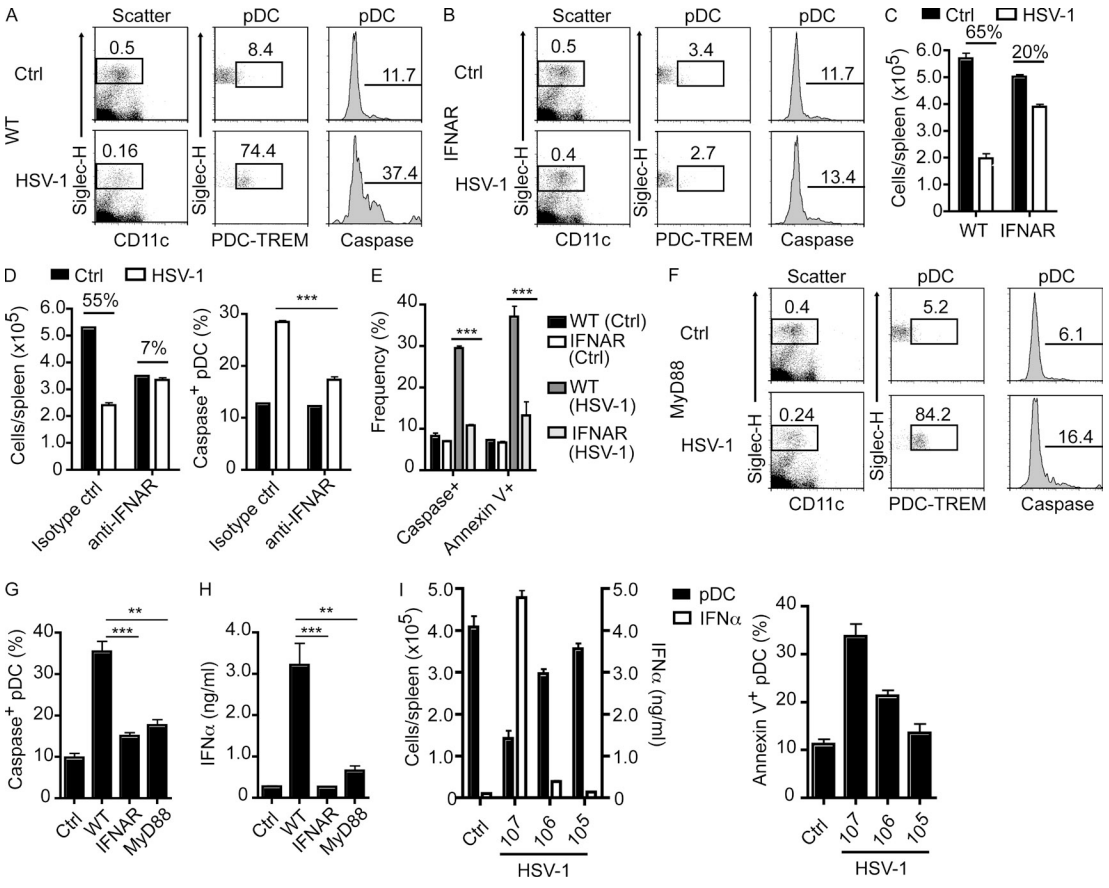

Figure 2. pDCs undergo cell death during systemic HSV-1 infection in an IFN-I–dependent manner. (A and B) C57BL/6 (A) and IFNAR$^{-/-}$ (B) mice were infected with 10^7 pfu HSV-1 for 8 h. Control mice were uninfected. pDC frequencies in spleens, expression of PDC-TREM, and caspase activation in pDCs were measured by flow cytometry. Dot plots and histograms show data from three to five mice per genotype representative of three experiments. (C) pDC numbers in spleens from C57BL/6 and IFNAR$^{-/-}$ mice infected or not with 10^7 pfu HSV-1 for 8 h. Data are representative of three experiments with three to five mice per group. Percentages denote the reduction in pDC numbers in infected mice relative to controls. (D) C57BL/6 mice were treated with an isotype control mAb or anti-IFNAR mAb 4 h before infection with 10^7 pfu HSV-1. Bar graphs show absolute numbers of pDCs (left) and frequencies of caspase$^+$ pDCs (right) in control and infected mice 8 h p.i. Data are representative of two experiments with three to four mice per group. Percentages indicate the reduction in pDC numbers in infected mice relative to controls. Statistical significance is indicated by ***, $P < 0.0001$. (E) C57BL/6 and IFNAR$^{-/-}$ mice were infected or not with 10^7 pfu HSV-1 for 8 h. Caspase$^+$ and Annexin V$^+$ pDCs were determined by flow cytometry. Data are representative of two experiments with three to four mice per group. Statistical significance is indicated by ***, $P \leq 0.0006$. (F) MyD88$^{-/-}$ mice were infected or not with 10^7 pfu HSV-1. pDC frequencies in spleens, expression of PDC-TREM, and caspase activation in pDCs were measured by flow cytometry 8 h p.i. Dot plots and histograms show data from three to five mice per group representative of two experiments. (G and H) Mice of the indicated genotype were infected or not with 10^7 pfu HSV-1 for 8 h. Bar graphs show frequencies of caspase$^+$ pDCs in spleens (G) and serum IFN-α levels (H). Data are combined from two experiments with four to eight mice per genotype. Statistical significance is indicated by **, $P < 0.007$; ***, $P < 0.0007$. (I) C57BL/6 mice were infected or not with different doses of HSV-1 (10^7, 10^6 or 10^5 pfu) for 8 h. pDC numbers in spleens, serum IFN-α levels, and Annexin V$^+$ pDCs were determined. Data are from representative of two experiments with three to four mice per group. (C–E and G–I) Error bars represent means ± SEM.

mice infected with HSV-1. Frequencies of caspase$^+$ and Annexin V$^+$ pDCs were significantly higher in infected WT mice compared with infected IFNAR$^{-/-}$ mice (Fig. 2 E). Collectively, these data show that pDC activation and death during systemic viral infection are dependent on IFN-I signaling.

To establish the impact of TLR signaling on pDC survival, we infected MyD88$^{-/-}$ mice i.v. with HSV-1. Infected MyD88$^{-/-}$ mice had an intermediate phenotype between that of infected WT and IFNAR$^{-/-}$ mice (Fig. 2 F). pDC frequencies were partially reduced compared with uninfected controls but not to the extent observed in WT mice. Similarly, minor fractions of pDC from HSV-1–infected MyD88$^{-/-}$ mice were caspase$^+$ compared with uninfected mice and to pDCs from infected WT mice. In contrast to IFNAR$^{-/-}$ pDCs, MyD88$^{-/-}$ pDCs up-regulated PDC-TREM during HSV-1 infection. The differences in caspase activation observed in pDCs from WT versus IFNAR$^{-/-}$ and MyD88$^{-/-}$ mice correlated with systemic IFN-α levels. On average, the frequencies of caspase$^+$ pDCs in WT mice approached 40%, compared with 14 and 20% in IFNAR$^{-/-}$ and MyD88$^{-/-}$ mice, respectively (Fig. 2 G). Following that trend, serum IFN-α levels in WT mice were ∼4.0 ng/ml, whereas IFNAR$^{-/-}$ and MyD88$^{-/-}$ mice had levels of ∼0.3 and 0.8 ng/ml, respectively (Fig. 2 H). Thus, during systemic HSV-1 infection, MyD88 signaling contributes in part to systemic IFN-α levels and pDC death but not to pDC activation as measured by PDC-TREM expression. Finally, we determined whether pDC survival was impacted by the dose of HSV-1 inoculum. As virus inoculum increased, pDC numbers declined, whereas serum IFN-α levels and Annexin V$^+$ pDCs increased (Fig. 2 I). These data indicate that pDC death correlates with viremia and systemic IFN-α levels.

Sources of IFN-I that promote pDC death

Given that pDCs are a source of IFN-I during HSV-1 infection (Krug et al., 2004), we asked whether caspase activation in pDCs is dependent on pDC-derived IFN-I and/or alternative IFN-I sources. Studies in pDC-depleted mice (Swiecki et al., 2010) revealed that pDCs are a major source of IFN-α early during HSV-1 infection but not at later time points (Fig. 3 A and not depicted), suggesting that pDCs produce the IFN-I that induces their death. To evaluate this, we looked at IFN-α levels and caspase activation in mice injected with the synthetic ligands CpGA and polyinosinic:polycytidylic acid (poly(I:C)). CpGA elicits IFN-I in pDCs through TLR9, whereas poly(I:C) induces IFN-I production from cDC and/or macrophages and stromal cells via TLR3 and MDA5, respectively (Gilliet et al., 2008; Longhi et al., 2009). We found that depleting pDCs has an impact on IFN-α production in response to CpGA but not poly(I:C) (Fig. 3 B), whereas administration of either ligand resulted in pDC activation and death (Fig. 3 C).

We next asked whether the direct administration of IFN-I impacts pDC numbers in vivo. To test this, WT and IFNAR$^{-/-}$ mice were injected with recombinant IFN-β and IFN-α5, and pDC numbers, as well as pDC expression of caspase and

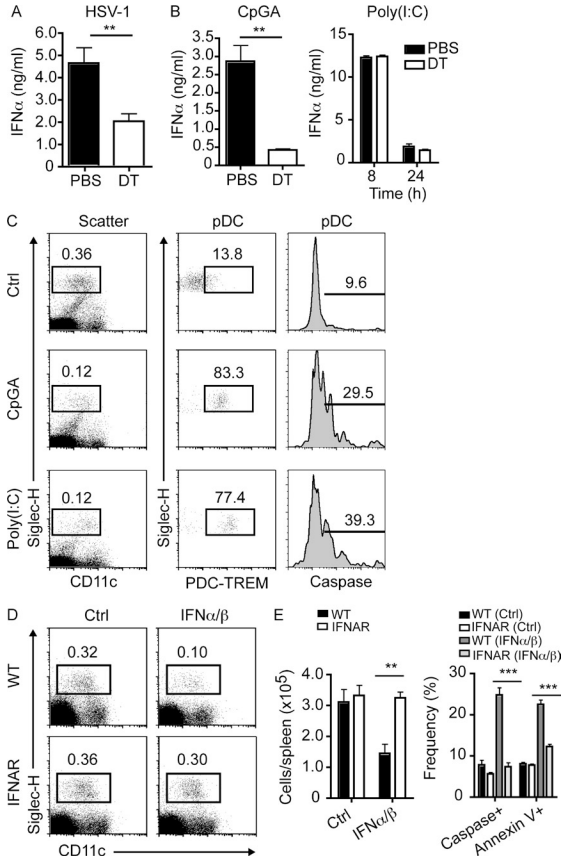

Figure 3. IFN-I–mediated death of pDCs does not depend on the IFN-I source. (A) BDCA2-DTR Tg mice were injected with PBS or DT before 10^7 pfu HSV-1. Serum IFN-α levels were measured by ELISA 6 h p.i. Data are combined from two experiments with five mice per group. (B) BDCA2-DTR Tg mice were injected with PBS or DT before CpGA or poly(I:C). Serum IFN-α levels were determined by ELISA 8 h after CpGA or 8 and 24 h after poly(I:C). Data are representative of two experiments with four to five mice per group. (C) BDCA2-DTR Tg mice were injected with CpGA or poly(I:C) and pDC frequencies in spleens, expression of PDC-TREM, and caspase activation were measured by flow cytometry 8 h after CpGA or 16 h after poly(I:C) administration. Dot plots and histograms show data from three to four mice per group representative of two experiments. Statistical significance is indicated by **, $P < 0.008$. (D and E) C57BL/6 and IFNAR$^{-/-}$ mice were injected with recombinant mouse IFN-I. (D) Dot plots show frequencies of pDCs in spleens 12 h after injection. (E) Absolute numbers of pDCs (left) as well as caspase$^+$ and Annexin V$^+$ pDCs in spleens (right) 12 h after injection. Data are representative of two experiments with three mice per group. Statistical significance is indicated by **, $P < 0.006$; ***, $P \leq 0.0008$. (A, B, and E) Error bars represent means ± SEM.

Annexin V, were determined. The frequencies and numbers of pDCs declined in IFN-I–treated WT mice but not IFNAR$^{-/-}$ mice (Fig. 3, D and E). Furthermore, we detected more caspase$^+$ and Annexin V$^+$ pDCs in WT mice treated with IFN-I compared with IFNAR$^{-/-}$ mice (Fig. 3 E). Thus, our findings indicate that although pDCs can be a source of IFN-I that induces pDC death, additional sources of endogenous, as well as exogenous, IFN-I can regulate pDC numbers in vivo.

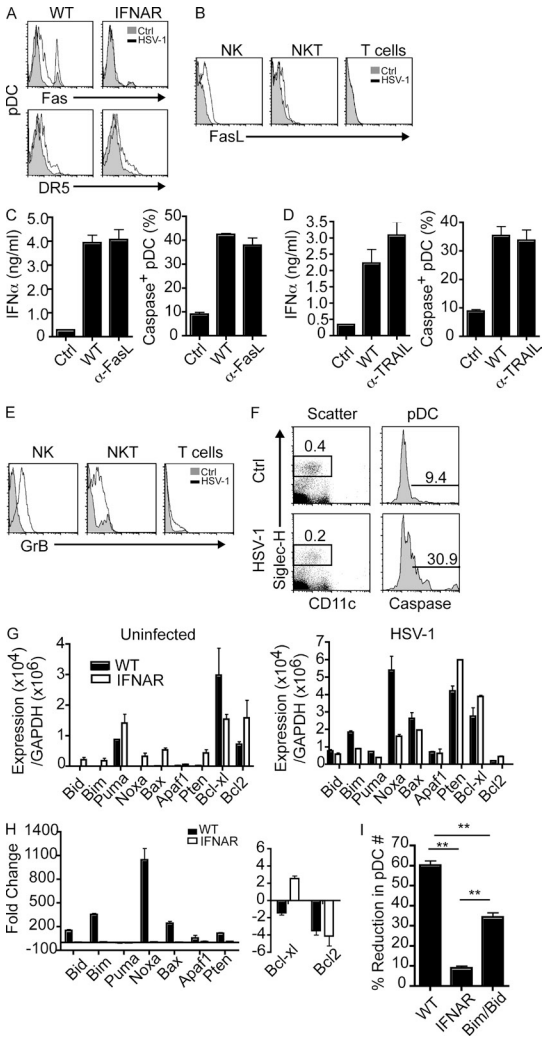

Figure 4. pDCs up-regulate extrinsic and intrinsic apoptotic proteins in an IFN-I–dependent manner during systemic HSV-1 infection. (A–I) Mice were infected or not with 10^7 pfu HSV-1. (A) Expression of Fas and DR5 on pDCs from spleens was determined 8 h p.i. Histograms show data from three to five mice per group from two experiments. (B) FasL expression on NK, NKT, and T cells from spleens of control and HSV-1–infected C57BL/6 mice 8 h p.i. Histograms show data from three to five mice per group from three experiments. (C) C57BL/6 mice were treated or not with anti-FasL mAb before HSV-1 infection. Bar graphs show serum IFN-α levels (left) and frequencies of caspase$^+$ pDCs (right) in spleens 8 h p.i. (D) C57BL/6 mice were treated or not with anti-TRAIL mAb before HSV-1 infection. Bar graphs show serum IFN-α levels (left) and frequencies of caspase$^+$ pDCs (right) in spleens 8 h p.i. (E) Granzyme B (GrB) expression on NK, NKT, and T cells from spleens of control and HSV-1–infected C57BL/6 mice 8 h p.i. Histograms show data from three to five mice per group from two experiments. (F) Mice were depleted of NK1.1$^+$ cells before HSV-1 infection. Dot plots show frequencies of pDCs and histograms show frequencies of caspase$^+$ pDCs in spleens 8 h p.i. Data are representative of two experiments with four mice per group. (G and H) C57BL/6 and IFNAR$^{-/-}$ mice were infected or not with HSV-1, RNA was isolated from pDCs sorted from spleens 4 h p.i., and relative levels of pro- and antiapoptotic molecules were measured in duplicate by qPCR. (G) Relative expression in naive (left) and HSV-1–infected (right) pDCs. (H) Fold change in WT and IFNAR$^{-/-}$ mice. (I) Absolute numbers of pDCs in spleens were determined in C57BL/6, IFNAR$^{-/-}$, and Bim/Bid$^{-/-}$ mice 8 h p.i. The bar graph shows the percent reduction in pDCs in HSV-1–infected mice compared with controls. Data are combined from two experiments with four mice per group. Statistical significance is indicated by **, $P < 0.005$. (C and D) Data are representative of two experiments with three to five mice per group. (G and H) Data are representative of two experiments where pDCs were sorted and pooled from three mice per genotype. (C, D, and G–I) Error bars represent means ± SEM.

pDC death occurs independently of the extrinsic apoptosis pathway

We next evaluated potential mechanisms leading to IFN-I–dependent caspase induction in pDCs. IFN-I induces the expression of Fas and TNF-related apoptosis-inducing ligand (TRAIL) which, through Fas/FasL and TRAIL/death receptor 5 (DR5) interactions, induce apoptosis via the extrinsic pathway. Using WT and IFNAR$^{-/-}$ mice infected i.v. with HSV-1, we found that a fraction of pDCs from WT, but not IFNAR$^{-/-}$, mice up-regulated Fas, whereas pDCs from both groups expressed very low levels of DR5 (Fig. 4 A). TRAIL and FasL were not clearly detectable on pDCs from any of the groups (unpublished data). FasL was detected at minimal levels on NK and NKT cells during HSV-1 infection (Fig. 4 B), which prompted us to examine whether caspase activation and pDC death might be mediated by Fas/FasL interactions with either NK or NKT cells. Disrupting Fas/FasL interactions by Ab blockade did not impact IFN-α responses to HSV-1 or prevent caspase activation in pDCs (Fig. 4 C).

Although we could not detect TRAIL on NK cells or pDCs, we attempted to block any potential TRAIL/DR5 interactions in vivo with an anti-TRAIL mAb before infecting mice with HSV-1. Blocking TRAIL had no impact on IFN-α production or caspase activation in pDCs (Fig. 4 D). We also asked whether NK or NKT cells might kill pDCs via perforin/granzyme, which can be induced by IFN-I during virus infections (García-Sastre and Biron, 2006). Although NK and NKT cells up-regulated granzyme B during HSV-1 infection (Fig. 4 E), depletion of NK1.1$^+$ cells before HSV-1 infection did not have an impact on pDC frequencies or caspase activation (Fig. 4 F). Collectively, these data suggest that pDC death is independent of Fas/FasL or TRAIL/DR5 interactions and NK or NKT cell cytolytic activity during HSV-1 infection.

Systemic HSV-1 infection induces pDC expression of proapoptotic molecules in an IFN-I–dependent manner

We next evaluated the expression of molecules involved in the intrinsic apoptosis pathway. The Bcl-2 family is composed of several proteins that exert either pro- or antiapoptotic functions (Youle and Strasser, 2008). To ascertain whether IFN-I induced the expression of proapoptotic molecules in pDCs during systemic HSV-1 infection, we isolated RNA from pDCs sorted from naive and HSV-1–infected WT and IFNAR$^{-/-}$ mice and then measured transcripts for pro- and antiapoptotic molecules by quantitative (q) PCR (Fig. 4 G).

We found that pDCs from infected WT mice strongly up-regulated Bid, Bim, Noxa, and Bax while down-regulating Bcl-xl and Bcl-2 compared with pDCs from naive WT mice (Fig. 4 H). In contrast, pDCs from infected IFNAR$^{-/-}$ mice displayed little to no change in the expression of proapoptotic molecules compared with pDCs from naive IFNAR$^{-/-}$ mice, although, they did increase their expression of Bcl-xl and decrease their expression of Bcl-2 (Fig. 4 H).

We then asked if pDCs from mice deficient for components of the intrinsic pathway were more resistant to apoptosis after HSV-1 infection. To test this, we infected WT, IFNAR$^{-/-}$, and Bim/Bid$^{-/-}$ mice with HSV-1 and determined pDC numbers 8 h p.i. pDC numbers were reduced 60% in WT mice and 8% in IFNAR$^{-/-}$ mice infected with HSV-1 (Fig. 4 I). In Bim/Bid$^{-/-}$ mice, pDC numbers were reduced 35%, indicating that in the absence of these two proapoptotic proteins pDC numbers were partially maintained. These data demonstrate that IFN-I generated during systemic HSV-1 infection induces the expression of proapoptotic molecules in pDCs leading to caspase activation and cell death. Deficiency in components of the intrinsic apoptosis pathway results in increased survival of pDCs during systemic HSV-1 infection.

Concluding remarks

In this study, we found that pDCs are reduced in vivo during several systemic viral infections. Mechanistically, we observed that IFN-I, regardless of the source, mediates pDC death in vivo by inducing the expression of proapoptotic molecules and caspase activation in pDCs. Previous studies have demonstrated that IFN-I signaling promotes the survival of mouse and human pDCs ex vivo, and activates pDCs and induces their migration in vivo (Kadowaki et al., 2000; Asselin-Paturel et al., 2001, 2005). Thus, the distinct outcomes of IFN-I signaling on pDCs suggest that pDC responses to IFN-I are influenced by the microenvironment. It has been shown that IFN-I regulates turnover of classical DCs in vivo by inducing the up-regulation of proapoptotic molecules and caspase activation (Mattei et al., 2009; Yen and Ganea, 2009; Fuertes Marraco et al., 2011). Impairment in DC turnover leads to increased numbers of DCs, chronic lymphocyte activation, and manifestations of autoimmunity (Nopora and Brocker, 2002; Chen and Wang, 2010). Similarly, the rapid turnover of pDCs during an IFN-I response in vivo may prevent excessive IFN-I–mediated cellular activation, immunopathology, and perhaps autoimmunity.

Our findings may explain the loss of pDCs during viral infections such as HIV, in which protracted deletion of pDCs might contribute to immunodeficiency. pDC numbers are reduced in patients with HIV but can be partially restored after antiretroviral therapy (HAART; Finke et al., 2004). Thus, HAART may reduce viral burden and systemic IFN-I levels improving the survival of pDCs during HIV infection (Boasso and Shearer, 2008). HIV infection may also affect pDC function or induce pDC anergy independently of IFN-I signaling, similar to what has been observed in experimental models of chronic viral infection with LCMV clone 13 (Zuniga et al., 2008; Lee et al., 2009). Current treatments for chronic Hepatitis C virus (HCV) infection include IFN-α in combination with ribavirin. Interestingly, it has been reported that blood pDCs are reduced in HCV patients receiving IFN-α therapy compared with untreated patients (Goutagny et al., 2004). Our findings suggest that treatment with IFN-I may also negatively regulate pDC numbers during human infections.

MATERIALS AND METHODS

Mice and treatments. All animal studies were approved by the Washington University Animal Studies Committee. IFNAR$^{-/-}$ mice (C57BL/6 background) were provided by A. French (Washington University, St. Louis, MO). Bim$^{-/-}$ and Bid$^{-/-}$ mice have been previously described (Bouillet et al., 1999; Kaufmann et al., 2007) and were provided by A. Strasser (Walter and Eliza Hall Institute, Victoria, Australia). C57BL/6, BDCA2-DTR Tg and 129/SvJ were bred in house. Heterozygous SiglecH-eGFP gene-targeted mice on a 129/SvJ background have been recently described and were bred in house (Swiecki et al., 2010). MyD88$^{-/-}$ mice (C57BL/6 background) were bred in house. All mice were used at 6–12 wk of age. Diphtheria toxin (DT; Sigma-Aldrich) was injected i.p. into BDCA2-DTR Tg mice (100–120 ng/mouse) 24 h before HSV-1, CpGA, or poly(I:C) administration. Approximately 200 µg PK136 mAb was injected i.p. 48 h before HSV-1 infection. Purified anti-FasL mAb (CD178, clone MFL3; BioLegend) or purified anti-TRAIL mAb (CD253, clone N2B2; BioLegend) were injected i.v. at 100 µg per mouse 20 h before HSV-1 infection. Anti-IFNAR and isotype control mAbs were injected i.v. at 625 µg per mouse 4 h before HSV-1. Recombinant mouse IFN-β and IFN-α5 were gifts from D. Fremont (Washington University, St. Louis, MO). Mice were injected i.v. with 15,000 U of both IFN-β and IFN-α5.

In vivo infections and stimulations. Kos strain HSV-1, Smith strain MCMV, MCMV AT1.5 (Δm157), Indiana strain VSV-OVA, LCMV clone 13, and VACV were provided by D. Leib (Dartmouth College, Hanover, NH), W. Yokoyama (Washington University, St. Louis, MO), A. French (Washington University, St. Louis, MO), L. Lefrançois (University of Connecticut, Farmington, CT), R. Ahmed (Emory University, Atlanta, GA), and L. Deng (Sloan-Kettering, New York, NY), respectively. Salivary gland stocks of MCMV and AT1.5 were administered i.p. HSV-1, and VSV-OVA, LCMV clone 13, and VACV were injected i.v. Administered doses of viruses are described in the figure legends. 6–9 µg CpGA 2216 (Operon) complexed with 30 µl DOTAP (Roche) was injected i.v. in phosphate-buffered saline. Poly(I:C) (GE Healthcare) was injected i.v. at 200 µg per mouse.

Cell preparations. Spleens were minced and digested for 45 min at 37°C in RPMI 1640 with collagenase D (Sigma-Aldrich). Single cell suspensions of spleens were prepared by passage through nylon mesh cell strainers (BD). EDTA was only used in MACS buffer for cell enrichment before sorting. Red blood cells were lysed with RBC lysis buffer (Sigma-Aldrich). Serum was separated from whole blood in serum collection tubes and stored at −20°C until analysis.

Antibodies, flow cytometry, and cell sorting. The following reagents were obtained from BD, eBioscience, or BioLegend. Fluorochrome labeled anti-SiglecH (551), anti-B220 (RA3-6B2), anti-CD11c (HL3), anti-Ly6C (AL-21), anti-CD3 (145-2C11), anti-NK1.1 (PK136), anti–Granzyme B (GB11), anti-CD262 (DR5, MD5-1), anti-CD178 (FasL, MFL3), anti-CD95 (Fas, clone 15A7), anti-CD253 (TRAIL, clone N2B2), and Streptavidin. Anti–PDC-TREM (clone 162.7, rat IgG2a) was purified from ascites and biotinylated using the FluoReporter Minibiotin kit (Invitrogen). Fc receptors were blocked before surface staining with supernatant from HB-197 cells (American Type Culture Collection). Propidium iodide was used to determine pDC frequencies and numbers during virus infections shown in Fig. 1. Propidium iodide was not used in caspase activation or Annexin V experiments. All flow cytometry was conducted on a dual laser FACSCalibur

flow cytometer (BD) and analyzed with FlowJo software (Tree Star). For pDC sorting from HSV-1–infected mice, $CD11c^+$ cells were enriched from spleens with anti–mouse CD11c microbeads as recommended by the manufacturer (Miltenyi Biotec). Cells were stained with anti–Siglec-H and anti-CD11c and then sorted on a FACSAria II high speed cell sorter (BD). Purities were always >98%.

Apoptosis and cytokine analysis. Spleens were harvested from control or manipulated mice and cell suspensions were prepared as described. After surface staining, cells were incubated with CaspACE FITC-VAD-FMK (Promega) or Annexin V (BD) as recommended by the manufacturer. Serum samples from infected mice were collected at various time points p.i. and IFN-α levels were determined by ELISA (PBL Interferon Source).

Tissue samples and immunohistochemistry. Spleens from eight mice/group (Ctrl and MCMV 36 h p.i.) were analyzed. 5-µm frozen tissue sections were used for immunohistochemical staining to visualize and count pDCs. For immunohistochemistry, sections were air dried overnight and fixed in acetone for 10 min. Non-specific binding was prevented using a protein block (Novocastra Laboratories) for 5 min. Incubation with purified 440c mAb (rat IgG2a) was followed by rat on mouse AP polymer kit (Biocare Medical) and revealed using Ferangi Blue Chromogen (Biocare Medical). The second immune reaction against CD3 antigen (rabbit monoclonal, clone SP7, dilution 1:100; Thermo Fisher Scientific) was visualized using Envision Rabbit-HRP (Dako) followed by DAB. Sections were slightly counterstained with Hematoxylin. For pDC counts, at least 30 high power fields of white pulp/spleen were counted on two distinct sections (200-µm distance) stained with 440c. Numbers are expressed as mean ± SD. Digital images were taken using a microscope (BX60; Olympus) and captured using a digital camera (DP-70; Olympus) and processed using Analysis Image Processing software (Olympus).

RNA preparation and qPCR. RNA was extracted from sorted pDCs using the RNeasy Micro kit (QIAGEN) as recommended by the manufacturer. cDNA was synthesized from RNA with Superscript III first-strand synthesis system for RT-PCR (Invitrogen), and relative levels of Bid, Bim, Puma, Noxa, Bax, Apaf1, Pten, Bcl-xl, and Bcl-2 were determined by qPCR. SYBR Green PCR master mix (Bio-Rad Laboratories) and an ABI7000 machine (Applied Biosystems) were used according to the manufacturer's instructions. PCR conditions were 2 min at 50°C and 10 min at 95°C, followed by 40 two-step cycles consisting of 15 s at 95°C and 1 min at 60°C. The values of each sample were normalized to GAPDH.

Statistical analysis. The statistical significance of differences in mean values was analyzed with an unpaired two-tailed Student's *t* test. P-values <0.05 were considered statistically significant.

We would like to thank Wayne Yokoyama, Anthony French, Theresa Geurs, Daved Fremont, Megan Epperson (Washington University, St. Louis, MO), Leo Lefrançois (University of Connecticut, Farmington, CT), and Andreas Strasser (Walter and Eliza Hall Institute, Australia) for reagents, animals and advice on virus infections; Silvia Lonardi and Elisa Bonomi for their technical support; and Olga Malkova and Danielle Atibalentja for cell sorting.

M. Swiecki was supported by the National Research Service Award training grant 5T32DK007296 from the National Institute of Diabetes and Digestive and Kidney Diseases. Y. Wang is supported by the Pulmonary and Critical Care training grant 2T32HL007317-31 from the National Heart, Lung and Blood Institute. W. Vermi is supported by a grant from Regione Lombardia "Call per la ricerca indipendente." This project was supported by the NIH grant R01 DE021255-01 and the National Institute of Allergy and Infectious Diseases Center for HIV/AIDS Vaccine Immunology grant A1067854.

The authors have no financial conflicts of interest.

Submitted: 1 April 2011
Accepted: 17 October 2011

REFERENCES

Altfeld, M., L. Fadda, D. Frleta, and N. Bhardwaj. 2011. DCs and NK cells: critical effectors in the immune response to HIV-1. *Nat. Rev. Immunol.* 11:176–186. http://dx.doi.org/10.1038/nri2935

Asselin-Paturel, C., A. Boonstra, M. Dalod, I. Durand, N. Yessaad, C. Dezutter-Dambuyant, A. Vicari, A. O'Garra, C. Biron, F. Brière, and G. Trinchieri. 2001. Mouse type I IFN-producing cells are immature APCs with plasmacytoid morphology. *Nat. Immunol.* 2:1144–1150. http://dx.doi.org/10.1038/ni736

Asselin-Paturel, C., G. Brizard, K. Chemin, A. Boonstra, A. O'Garra, A. Vicari, and G. Trinchieri. 2005. Type I interferon dependence of plasmacytoid dendritic cell activation and migration. *J. Exp. Med.* 201:1157–1167. http://dx.doi.org/10.1084/jem.20041930

Boasso, A., and G.M. Shearer. 2008. Chronic innate immune activation as a cause of HIV-1 immunopathogenesis. *Clin. Immunol.* 126:235–242. http://dx.doi.org/10.1016/j.clim.2007.08.015

Bouillet, P., D. Metcalf, D.C. Huang, D.M. Tarlinton, T.W. Kay, F. Köntgen, J.M. Adams, and A. Strasser. 1999. Proapoptotic Bcl-2 relative Bim required for certain apoptotic responses, leukocyte homeostasis, and to preclude autoimmunity. *Science.* 286:1735–1738. http://dx.doi.org/10.1126/science.286.5445.1735

Brown, K.N., V. Wijewardana, X. Liu, and S.M. Barratt-Boyes. 2009. Rapid influx and death of plasmacytoid dendritic cells in lymph nodes mediate depletion in acute simian immunodeficiency virus infection. *PLoS Pathog.* 5:e1000413. http://dx.doi.org/10.1371/journal.ppat.1000413

Chen, M., and J. Wang. 2010. Programmed cell death of dendritic cells in immune regulation. *Immunol. Rev.* 236:11–27. http://dx.doi.org/10.1111/j.1600-065X.2010.00916.x

Duan, X.Z., M. Wang, H.W. Li, H. Zhuang, D. Xu, and F.S. Wang. 2004. Decreased frequency and function of circulating plasmocytoid dendritic cells (pDC) in hepatitis B virus infected humans. *J. Clin. Immunol.* 24:637–646. http://dx.doi.org/10.1007/s10875-004-6249-y

Finke, J.S., M. Shodell, K. Shah, F.P. Siegal, and R.M. Steinman. 2004. Dendritic cell numbers in the blood of HIV-1 infected patients before and after changes in antiretroviral therapy. *J. Clin. Immunol.* 24:647–652. http://dx.doi.org/10.1007/s10875-004-6250-5

Fonteneau, J.F., M. Larsson, A.S. Beignon, K. McKenna, I. Dasilva, A. Amara, Y.J. Liu, J.D. Lifson, D.R. Littman, and N. Bhardwaj. 2004. Human immunodeficiency virus type 1 activates plasmacytoid dendritic cells and concomitantly induces the bystander maturation of myeloid dendritic cells. *J. Virol.* 78:5223–5232. http://dx.doi.org/10.1128/JVI.78.10.5223-5232.2004

Fuertes Marraco, S.A., C.L. Scott, P. Bouillet, A. Ives, S. Masina, D. Vremec, E.S. Jansen, L.A. O'Reilly, P. Schneider, N. Fasel, et al. 2011. Type I interferon drives dendritic cell apoptosis via multiple BH3-only proteins following activation by PolyIC in vivo. *PLoS ONE.* 6:e20189. http://dx.doi.org/10.1371/journal.pone.0020189

García-Sastre, A., and C.A. Biron. 2006. Type 1 interferons and the virus-host relationship: a lesson in détente. *Science.* 312:879–882. http://dx.doi.org/10.1126/science.1125676

Gilliet, M., W. Cao, and Y.J. Liu. 2008. Plasmacytoid dendritic cells: sensing nucleic acids in viral infection and autoimmune diseases. *Nat. Rev. Immunol.* 8:594–606. http://dx.doi.org/10.1038/nri2358

Goutagny, N., C. Vieux, E. Decullier, B. Ligeoix, A. Epstein, C. Trepo, P. Couzigou, G. Inchauspe, and C. Bain. 2004. Quantification and functional analysis of plasmacytoid dendritic cells in patients with chronic hepatitis C virus infection. *J. Infect. Dis.* 189:1646–1655. http://dx.doi.org/10.1086/383248

Kadowaki, N., S. Antonenko, J.Y. Lau, and Y.J. Liu. 2000. Natural interferon α/β–producing cells link innate and adaptive immunity. *J. Exp. Med.* 192:219–226. http://dx.doi.org/10.1084/jem.192.2.219

Kanto, T., M. Inoue, H. Miyatake, A. Sato, M. Sakakibara, T. Yakushijin, C. Oki, I. Itose, N. Hiramatsu, T. Takehara, et al. 2004. Reduced numbers and impaired ability of myeloid and plasmacytoid dendritic cells to polarize T helper cells in chronic hepatitis C virus infection. *J. Infect. Dis.* 190:1919–1926. http://dx.doi.org/10.1086/425425

Kaufmann, T., L. Tai, P.G. Ekert, D.C. Huang, F. Norris, R.K. Lindemann, R.W. Johnstone, V.M. Dixit, and A. Strasser. 2007. The BH3-only protein bid is dispensable for DNA damage- and replicative

stress-induced apoptosis or cell-cycle arrest. *Cell.* 129:423–433. http://dx.doi.org/10.1016/j.cell.2007.03.017

Krug, A., G.D. Luker, W. Barchet, D.A. Leib, S. Akira, and M. Colonna. 2004. Herpes simplex virus type 1 activates murine natural interferon-producing cells through toll-like receptor 9. *Blood.* 103:1433–1437. http://dx.doi.org/10.1182/blood-2003-08-2674

Lee, L.N., S. Burke, M. Montoya, and P. Borrow. 2009. Multiple mechanisms contribute to impairment of type 1 interferon production during chronic lymphocytic choriomeningitis virus infection of mice. *J. Immunol.* 182:7178–7189. http://dx.doi.org/10.4049/jimmunol.0802526

Longhi, M.P., C. Trumpfheller, J. Idoyaga, M. Caskey, I. Matos, C. Kluger, A.M. Salazar, M. Colonna, and R.M. Steinman. 2009. Dendritic cells require a systemic type I interferon response to mature and induce $CD4^+$ Th1 immunity with poly IC as adjuvant. *J. Exp. Med.* 206:1589–1602. http://dx.doi.org/10.1084/jem.20090247

Malleret, B., B. Manéglier, I. Karlsson, P. Lebon, M. Nascimbeni, L. Perié, P. Brochard, B. Delache, J. Calvo, T. Andrieu, et al. 2008. Primary infection with simian immunodeficiency virus: plasmacytoid dendritic cell homing to lymph nodes, type I interferon, and immune suppression. *Blood.* 112:4598–4608. http://dx.doi.org/10.1182/blood-2008-06-162651

Mattei, F., L. Bracci, D.F. Tough, F. Belardelli, and G. Schiavoni. 2009. Type I IFN regulate DC turnover in vivo. *Eur. J. Immunol.* 39:1807–1818. http://dx.doi.org/10.1002/eji.200939233

Nopora, A., and T. Brocker. 2002. Bcl-2 controls dendritic cell longevity in vivo. *J. Immunol.* 169:3006–3014.

Swiecki, M., S. Gilfillan, W. Vermi, Y. Wang, and M. Colonna. 2010. Plasmacytoid dendritic cell ablation impacts early interferon responses and antiviral NK and CD8(+) T cell accrual. *Immunity.* 33:955–966. http://dx.doi.org/10.1016/j.immuni.2010.11.020

Trinchieri, G. 2010. Type I interferon: friend or foe? *J. Exp. Med.* 207:2053–2063. http://dx.doi.org/10.1084/jem.20101664

Villadangos, J.A., and L. Young. 2008. Antigen-presentation properties of plasmacytoid dendritic cells. *Immunity.* 29:352–361. http://dx.doi.org/10.1016/j.immuni.2008.09.002

Watarai, H., E. Sekine, S. Inoue, R. Nakagawa, T. Kaisho, and M. Taniguchi. 2008. PDC-TREM, a plasmacytoid dendritic cell-specific receptor, is responsible for augmented production of type I interferon. *Proc. Natl. Acad. Sci. USA.* 105:2993–2998. http://dx.doi.org/10.1073/pnas.0710351105

Yen, J.H., and D. Ganea. 2009. Interferon beta induces mature dendritic cell apoptosis through caspase-11/caspase-3 activation. *Blood.* 114:1344–1354. http://dx.doi.org/10.1182/blood-2008-12-196592

Youle, R.J., and A. Strasser. 2008. The BCL-2 protein family: opposing activities that mediate cell death. *Nat. Rev. Mol. Cell Biol.* 9:47–59. http://dx.doi.org/10.1038/nrm2308

Zuniga, E.I., L.Y. Liou, L. Mack, M. Mendoza, and M.B. Oldstone. 2008. Persistent virus infection inhibits type I interferon production by plasmacytoid dendritic cells to facilitate opportunistic infections. *Cell Host Microbe.* 4:374–386. http://dx.doi.org/10.1016/j.chom.2008.08.016